Bactericidal and Fungicidal Action of Copper Nanoparticles on Leather Surface

by
Deepak N, Inbasekar C, Nishad Fathima Nishter*
Inorganic and Physical Chemistry Laboratory, CSIR-Central Leather Research Institute, Adyar, Chennai-600020

Abstract

Although tanning makes the collagen matrix resilient against microbial attack, the chemicals used in the finishing process are susceptible to microbes. Hence, it is imperative to develop a finishing process with inherent antimicrobial properties. Leathers with antimicrobial properties evoke a considerable array of interest in consumers. The present study aims to enhance the antimicrobial properties of the leather using copper nanoparticles in the finishing and retanning process. Copper nanoparticles have been synthesized by chemical reduction using copper sulphate pentahydrate as the precursor with dialdehyde starch and gallic acid. The prepared nanoparticles have been characterized using UV-Visible spectrometry, dynamic light scattering, scanning electron microscopy, transmission electron microscopy, and X-ray diffraction techniques. The prepared nanoparticles have been used in both retanning and finishing processes. The experimental leather retanned using copper nanoparticles possess good mechanical strength properties and color index value compare to the control. Nanoparticles are effective against both gram negative and positive bacterial organisms. The nanoparticles also inhibit the growth of common fungus, which can colonize on leather. Thus, the current study paves the way for a novel solution that is an alternative to biocides and antimicrobial chemicals and is more effective in inhibiting microbial growth.

1 Introduction

The extracellular matrix is a natural barrier that protects against invading microbes and other external factors. Collagen is the major protein in the extracellular matrix that provides structural integrity to the skin and is commonly known as leather making protein.[1] The leather process comprises pretanning, tanning, post tanning, and finishing. The post-tanning process imparts functional properties to the tanned leather by employing polymeric fillers, dyes, and lubricating agents. The selection of the post tanning process relies on the end product.[2] The finishing process enhances the aesthetic value and imparts other functional properties such as the leather's super hydrophobicity and antimicrobial properties. To prevent the growth of microbes in leather products, biocides and antimicrobial chemicals are widely used in the finishing process.[3]

The presence of microorganisms on the leather surface causes deterioration of raw materials at various stages of tanning or visible defects in finished leathers.[3] Especially vegetable-tanned leather is prone to microbial attack.[4] Fungi and bacteria also colonize finished products.[4] Sweat from footwear and lining in socks in shoe materials will be a carbon source for microbial growth.[5]

Several antimicrobial compounds have been utilized in the leather industry; however, some of these materials are ineffective owing to their composition, high cost, and pose a pollution risk, thereby limiting their application.[6] The use of biocides endangers the health of humans, animals, and the natural environment.[7] Metallic nanoparticles have distinct toxicity mechanisms in different microorganisms. The majority of metal oxides are lethal to all types of bacterial cells.[8] Some transition elements and coinage metals have all been found to have antibacterial properties.[9] For ages, copper and its compounds have been employed as disinfectants.[10] Many studies have been carried out on the antibacterial effects of metals such as copper as a result of research into the creation of antimicrobial agents, particularly antibacterial agents.[11] Copper nanoparticles cause plasmid DNA degradation in gram-positive and gram-negative pathogens in a dose-dependent manner.[12] Contact kills bacteria, yeasts, and viruses on copper surfaces.[13]

Copper nanoparticles can provide site-specific and targeted reactivity owing to their smaller sizes and large surface area, which promotes their penetration inside the bacterial cell.[14] The reduction of copper ions causes cascade events such as DNA degradation and the generation of Reactive Oxygen Species (ROS), which induces cell death by membrane damage.[15,16] Thus, the current study explores the antimicrobial properties of copper nanoparticles in the post tanning and finishing process.

2 Experimental

2.1 Materials

Copper sulphate pentahydrate, gallic acid monohydrate, polyethyleneimine (PEI), sodium periodate, sodium borohydride, 3,3'diphenylthiocarbocyanineiodide,2,7dichlorodihydrofluorescein diacetate (DCFHDA) were purchased from Sigma Aldrich. Mueller hinton agar (MHA), nutrient broth (NB), sabouraud dextrose agar (SDA), and potato dextrose broth (PDB) were purchased from

*Corresponding author email: nishad@clri.res.in or nishad.naveed@gmail.com
Manuscript received June 6, 2023, accepted for publication July 23, 2023.

HiMedia. Experiments were carried out by using analytical-grade chemicals. Two Gram-positive (*Staphylococcus aureus* and *Bacillus cereus*) and two gram-negative (E*scherichia coli* and *Pseudomonas aeruginosa*) bacterial strains and a fungal strain (A*spergillus niger*) were obtained from the MTCC. All the chemicals used for leather processing were of analytical grade. The chrome tanned wet blue goat leather and goat crust leather was collected from the Tannery division of CSIR-Central Leather Research Institute.

2.2. Methods

2.2.1. Preparation of Dialdehyde starch (DAS)

The dialdehyde starch was prepared using the standard procedure. About 20 g of corn starch and 10 g of sodium periodate (1:0.5) were dissolved in 100 ml of water in a round bottom flask with vigorous stirring at 37°C for 12 h. Then 5 ml of propylene glycol was added to the reaction mixture to quench the reaction. The resulting slurry was filtered and washed with water thrice and freeze-dried. The dialdehyde starch powder was used without further purification.

2.2.2. Synthesis of Copper nanoparticles

Copper nanoparticles were synthesized by the chemical reduction method. Copper sulphate pentahydrate was used as a precursor, with dialdehyde starch as a reducing agent and polyethyleneimine as a capping agent. Dialdehyde starch (DAS) solution was prepared by adding NaOH, Urea, and DAS (3:2:1) in water and 2% of this solution was cooled to -20°C for 12 h and thawed under stirring at room temperature. $CuSO_4$ solution (15 mM) 1 mL was taken in the round bottom flask and 5 mL of DAS solution and 1mL of polyethyleneimine (PEI) was added to this under magnetic stirring. The reaction mixture was thoroughly stirred and passed through N_2, and the round bottom flask was placed in an oil bath at 50°C for 3 h. Copper nanoparticles were synthesized using dialdehyde starch and polyethyleneimine as a reducing and capping agent, respectively. Dialdehyde starch was dissolved in NaOH/urea system to form a light-yellow colored solution. As the reaction proceeded, the mixture showed a gradual color change from light yellow to reddish-brown. After washing and purification, a reddish-brown solution was obtained. The resultant copper nanoparticles were freeze-dried and used without further purification.

For the retanning process, copper nanoparticles were synthesized using sodium borohydride and gallic acid. $CuSO_4$ solution (5 mM) 10 mL was thoroughly mixed with 10 mL (5mM) of gallic acid solution. Then 30 mL (10 mM) of $NaBH_4$ solution was added dropwise into the above mixture for 2 h in the dark. The obtained copper nanoparticles solution was further purified by centrifugation at 15,000 rpm for 20 minutes. The resultant copper nanoparticles were freeze-dried and used without further purification.

2.2.3. Characterization of Copper Nanoparticles

FTIR measurements were performed using an infrared spectrometer (JASCO IR). Infrared spectra were taken with a scan range of 400-4,000 cm^{-1}, and resolution of 4 cm^{-1}. Particle size and zeta potential analysis were performed using a high-performance particle analyzer (Zetasizer Nano series, Malvern) at 25°C. The samples were dissolved in a water medium for measurements. X'Pert Powder X-Ray Diffraction obtained the crystallographic studies and diffraction peaks. The samples were analyzed by powder diffraction using samples prepared as finely ground powders. An FEI Quanta 200 scanning electron microscope was used to study the morphological characteristics, and all specimens were then coated with gold using a palaron range CA7620-sputtering coater. Energy dispersive X-Ray was used to study the elemental composition of the nanoparticles. Fluorescence spectra were recorded on a Cary eclipse fluorescence spectrophotometer using quartz cuvettes at room temperature. BET-specific surface determination was based on an N_2 isothermal measurement at 77 K performed with an IMI-HTP manometric sorption analyzer (Hiden Isochema, Inc). Before the measurements, the samples were degassed at 420 K for 16 h. Transmission electron microscopy (TEM) samples were prepared by casting a drop of the as-prepared copper nanoparticle suspension on a carbon-coated copper grid and then drying them in air. The dried grid was placed under a JEOL 1200 EX transmission electron microscope. The images were taken at an acceleration voltage of 120 kV.

2.2.4. Finishing process

Goat crust leather was used for spray coating using High-Volume-Low-Pressure (HVLP) gun. A mixture of isopropyl alcohol and water was sprayed as a clear coat to remove the dust and increase the finishing formulation's penetration. Base coat formulation was prepared, and two cross coats were sprayed and dried. Top coat formulation with lacquer, copper nanoparticles, and water were prepared, and one cross coat was sprayed on the leather surface.

2.2.5. Post tanning leather process

Chrome tanned wet blue leather was used for retanning process, pH of the leather was adjusted to pH 5.5. Copper nanoparticles synthesized using gallic acid was used for the retanning process.

2.2.6. Characterization of Leather

The color values L*, a*, b* were determined using UV-Vis-NIR spectrophotometer Agilent CARY-5000. Tensile and tear strength was tested according to SATRA TM 43 and 162. The wet and dry rub fastness test was measured according to IUF 450 by veslic C-4500. Measurement of color fastness to water was carried out by SATRA TM 335-1.

2.2.7. Antibacterial Activity of Copper Nanoparticles

The antibacterial activity of synthesized copper nanoparticles and coated leather was assessed using the agar diffusion method. The bacterial culture broth was prepared by inoculating the bacterial strains in nutrient broth and allowed to grow overnight at 37°C. Two Gram-positive (*Staphylococcus aureus* and *Bacillus cereus*) and two gram-negative (*Escherichia coli* and *Pseudomonas aeruginosa*) bacterial strains were cultured. Mueller Hinton Agar was prepared

and poured into the sterile petri dish, and the bacterial strains at $1x10^6$ CFU/mL concentration were uniformly spread on plates using sterilized cotton swabs. Then the wells were made on the inoculated plates using a sterile gel borer. Wells were filled with 100 *μL of* different concentrations of synthesized copper nanoparticles (10, 20, 30, and 40 %), and the plates were incubated overnight at 37°C. The antibacterial activity of copper nanoparticles coated leather was assessed by placing the sample cut with a 2 cm radius compared with control leather.

2.2.8. Antifungal Activity of Copper Nanoparticles

The fungal culture broth was prepared by inoculating the fungal strain in potato dextrose broth and allowed to grow for 72 h at 28°C. A fungal strain (*Aspergillus niger*) was cultured. Sabouraud dextrose agar media was prepared and poured into a sterile petri dish, and the fungal strain at $1x10^6$ CFU/mL concentration was uniformly spread on plates using sterilized cotton swabs. Then the wells were made on the inoculated plates using a sterile gel borer. Wells were filled with 100 *μL of* 40 % of synthesized copper nanoparticles and the plates were incubated overnight at 37°C. The antifungal activity of copper nanoparticles coated leather was assessed by placing the sample cut with a 2 cm radius compared with control leather.

2.2.9. Determination of Membrane Potential of Intact E. coli *Cells*

The membrane potential of bacterial cell was determined by spectrofluorimetric methods, using the dye 3', 3'diphenylthiocarbocyanine iodide. To carry out the experiments, synchronized cells of *E. coli* were newly grown to the log phase in Luria–Bertani (LB) medium. The grown cells were then treated with 3.0 μg/mL CuNPs (the minimum inhibitory concentration (MIC)) for 1 h, centrifuged at 8000 rpm for 5 min, and the cell pellets were resuspended in starvation buffer (SB). As negative and positive controls, cells alone and cells treated with 3.0 μg/mL $CuSO_4$ (the precursor of the NPs) were also taken.

2.2.10. Determination of the Production of Reactive Oxygen Species (ROS) in E. coli *cells*

ROS production in bacterial cells was estimated using the chemical 2', 7' dichlorodihydrofluorescein diacetate (DCFHDA) as a marker to visualize the bacterial cell. Log phase grown cells, were prepared by treating with 3.0 μg/ml CuNPs for 1 h, centrifuged, and suspended in saline (8.0 g/L NaCl, 0:2 g/L KCl). The negative and positive control experiments were also done. The probe (1 μl of 10 mM DCFHDA) was added to each of the four sets and incubated for 2 h at ambient temperature in the dark. The fluorescence of each sample was then measured in the spectrofluorometer with excitation and emission wavelengths of 485 and 530 nm, respectively.

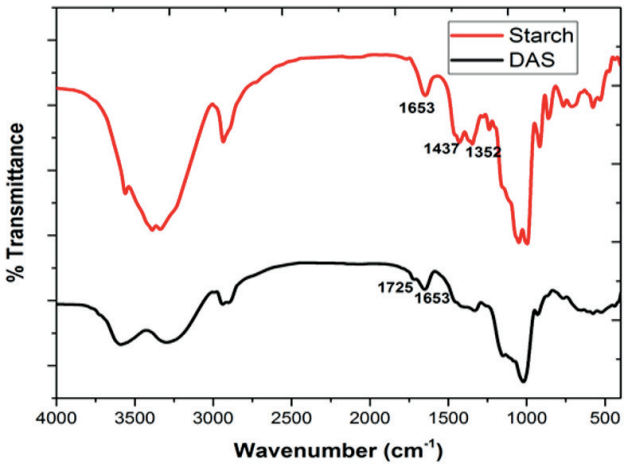

Figure 1. FT-IR Spectra of Starch and DAS (Dialdehyde starch)

3 Results and Discussion

IR spectroscopy has been used to study the functional groups present in the starch and dialdehyde starch. Figure 1 shows the FTIR spectra of starch and dialdehyde starch. The periodate oxidation of starch is characterized by the targeted cleavage of the C2-C3 bond of glucose residues in the starch.[17] The characteristics band at 1352 cm^{-1} corresponds to the C-H alkane bending and the band at 1725 cm^{-1} corresponds to the stretching vibration of the carbonyl C=O bond confirms the presence of aliphatic aldehyde group.[17] The results confirm the aldehyde group modification in the starch.

UV-Visible spectroscopy has been used to elucidate the formation of the nanoparticle. Nanoparticles size and shape are regulated by the precursor choice and the reaction conditions. For instance,

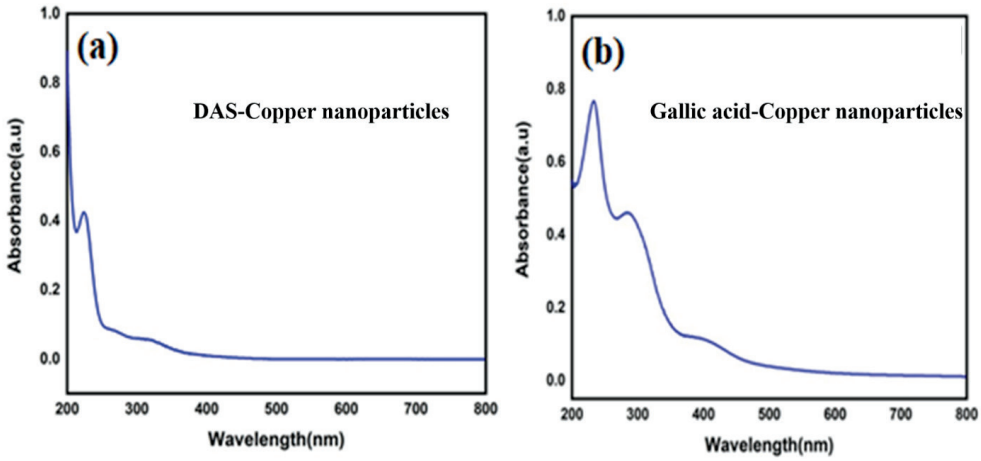

Figure 2. UV-Visible spectra of copper nanoparticles using (a) DAS and (b) gallic acid

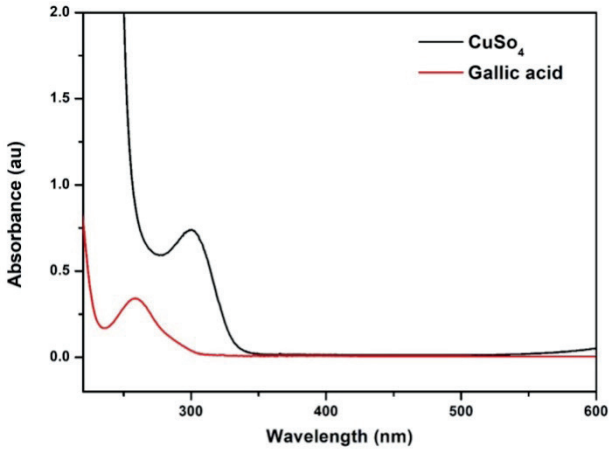

Figure S1. UV-Visible spectra of copper sulphate and gallic acid

the peaks of copper oxide nanoparticles usually occur in the 220–350 nm range and is attributed to Cu^{2+}–O– charge transfer transitions.[18] The copper nanoparticles synthesized using DAS exhibit a maximum absorption peak at approximately 253 nm, corresponding to a characteristic Cu nanoparticle peak (Figure 2 a).[20] The peak at 290 nm corresponds to the n→π* transition due to the presence of the carboxylic group of gallic acid.[22,23] The UV-Visible spectra of copper sulphate and gallic acid are given in supporting information (Figure S1).

Dynamic light scattering measurement has been performed to measure the nanoparticles' hydrodynamic diameter and surface charge. From Figure 3 (a) and (b), copper nanoparticles synthesized using DAS and PEI has a hydrodynamic diameter value of 105 ± 5 nm, PDI value of 0.325 and nanoparticles synthesized using sodium borohydride and gallic acid have a hydrodynamic diameter value of 280 ± 14 nm, PDI value of 0.387, respectively. The zeta potential of copper nanoparticles synthesized using DAS and PEI is 24.2 ± 1 mV and -38.8 ± 1.5 mV, respectively. The increase in D_H and ζ indicates that the presence of gallic acid influences the nanoparticle size and provides more stability to the nanoparticles. The negative zeta potential of copper nanoparticles synthesized using gallic acid is due to the presence of the deprotonated carboxyl group.

X-ray diffraction pattern measurement have been performed for copper nanoparticles synthesized using dialdehyde starch and gallic acid. Figure 4 (a) shows the major diffraction peaks at 2θ = 42.8°, 52.4°, 70.2° are assigned to be Miller indices plane (111), (200), and (220) correspond to the crystal planes of copper nanoparticles[19] and the Figure 4 (b) 2θ values 46.2°, 53.6°, which are indexed to planes (111), (200) has the significant variation in the crystallinity of copper nanoparticles due to the presence of gallic acid.[19]

The morphology of PEI stabilized Cu NPs was examined by FESEM. Figures 5 a and b show the fast emission SEM image of the spherical copper NPs, which are consistently dispersed due to the presence of capping agent PEI, which prevents the aggregation of the nanoparticles and results in uniform particle size.[24,25] EDAX

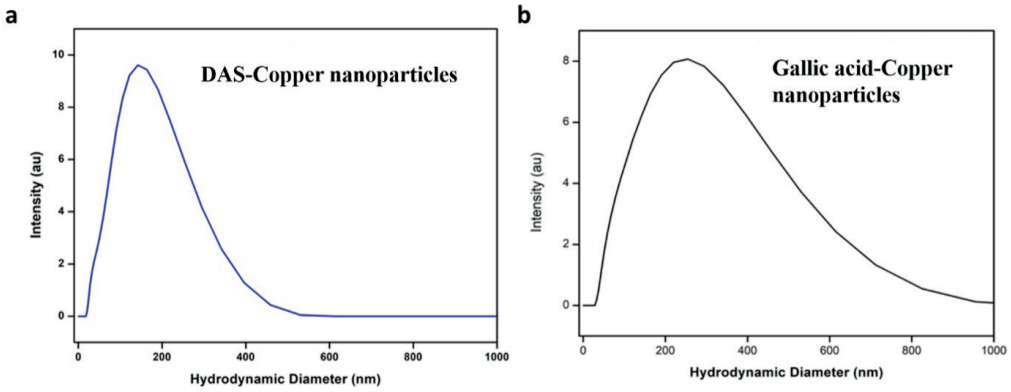

Figure 3. Particle size of copper nanoparticles using (a) DAS and (b) gallic acid

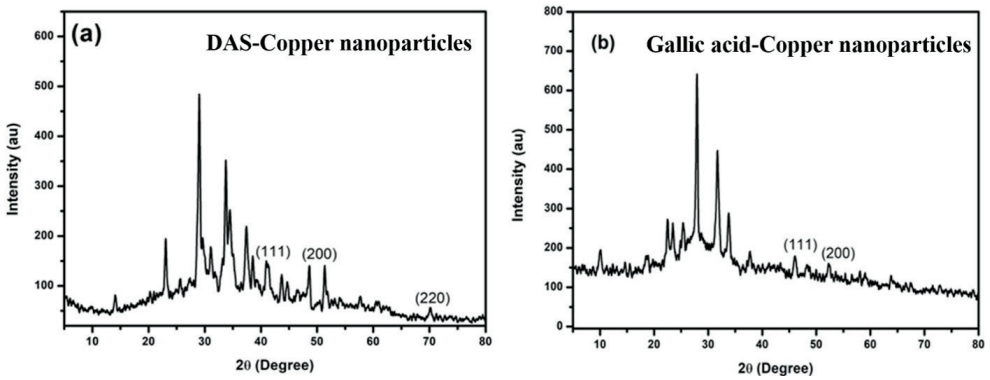

Figure 4. XRD pattern of copper nanoparticles using (a) DAS and (b) gallic acid

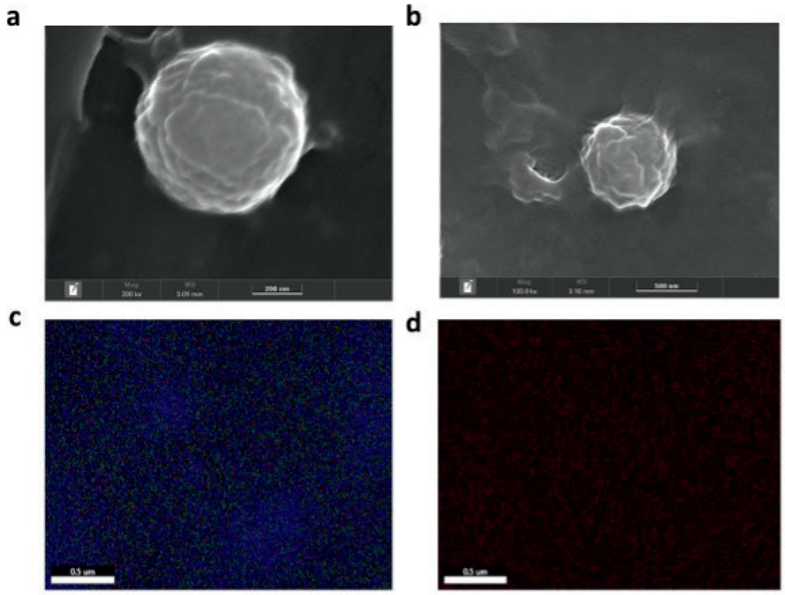

Figure 5. FESEM images of copper nanoparticles at magnification (a) 200 nm (b) 500 nm (c) overall E-DAX mapping of copper nanoparticles, (d) Copper E-DAX mapping of copper nanoparticles

mapping of copper nanoparticles are shown in Figures 5 c and d. Figure 5 c shows the overall mapping of copper nanoparticles with an elemental composition of carbon, nitrogen, oxygen and copper. Figure 5 d copper mapping shows the uniform distribution of copper in the synthesized nanoparticles.

Using TEM, the size and morphology of copper nanoparticles has been investigated. TEM images (Figure 6) further confirmed that the nucleation and growth of copper nanoparticles progressed with the reaction time. Most of the nanoparticles show contrast regions within one nanoparticle, indicating their polycrystalline structure spots confirm the presence of copper nanoparticles, and the results support the XRD pattern and SEM.

The Brunauer–Emmett–Teller (BET) analysis has been measured to assess the surface area molecules in the pores of nanoparticles.[15] The specific surface area and pore size distribution of copper nanoparticles has been measured by nitrogen adsorption/desorption at 77 K. The N_2 adsorption–desorption isotherms of copper nanoparticle samples, belonged to type II adsorption isotherms with flatter region in the middle represents the monolayer formation, indicating the presence of mesopores (6.7702 nm) and multilayer adsorption where the amount of adsorption increases with increase in pressure are shown for copper nanoparticles in Figure 7.[26] The BET surface area of the copper nanoparticles is 20 m^2g^{-1}. The most abundant pore size for the copper nanoparticles is the range of 2-10 nm also confirms the mesoporous nature of the nanoparticles.

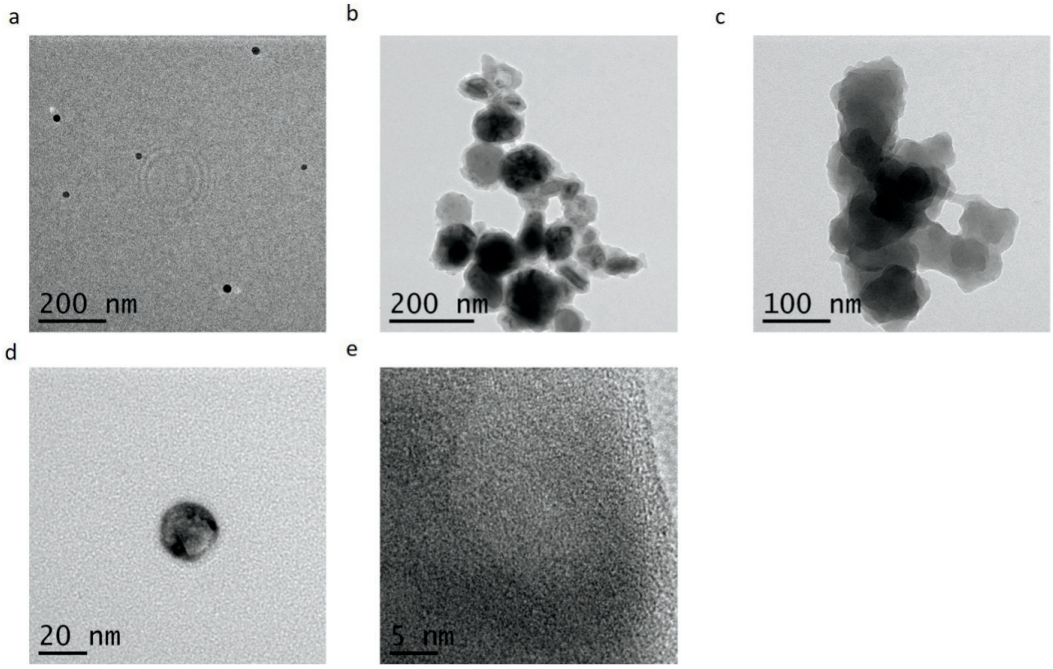

Figure 6. HRTEM images of copper nanoparticles at different magnifications (a) 200 nm (b) 200 nm (c) 100 nm (d) 20 nm (e) 5 nm

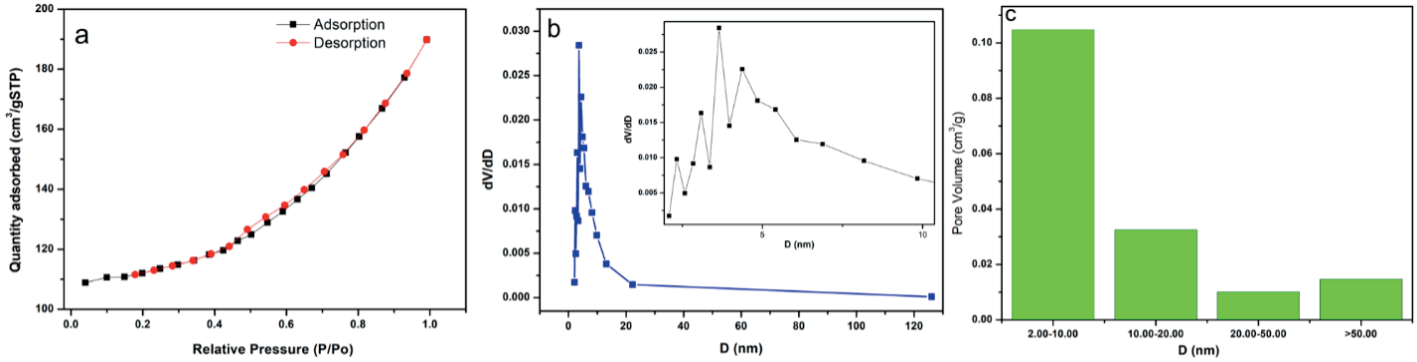

Figure 7. (a) Adsorption Desorption isotherm of copper nanoparticles (b) BJH Adsorption pore size of copper nanoparticles and (c) Pore volume of copper nanoparticles

The copper nanoparticles synthesized using sodium borohydride and gallic acid has been used in the retanning process. Figure 8 shows the photographic images of control retanned leather and copper nanoparticles incorporated in retanned leather. The leather retanned with copper nanoparticles shows high color intensity due to the presence of gallic acid. Gallic acid is used to functionalize the copper nanoparticles, thereby increasing the leather matrix's reactive sites and enhancing dye uptake in the experiment. Tables I and IV show the color fastness values of control and copper incorporated retanned leather; the color rub fastness ratings of both leathers are similar. After 256 and 512 cycles, it is found that both the leathers have excellent color rub fastness properties. From Table III, it could be observed that the physical strength properties exhibit a significant difference compared to the control leather. The experimental leather's organoleptic properties are relatively better than the control leather. The leaching studies were performed at regular intervals to check the copper nanoparticles leaching, and there was no leaking of nanoparticles after 24 h; the result is given in the supporting information (Figure S2).

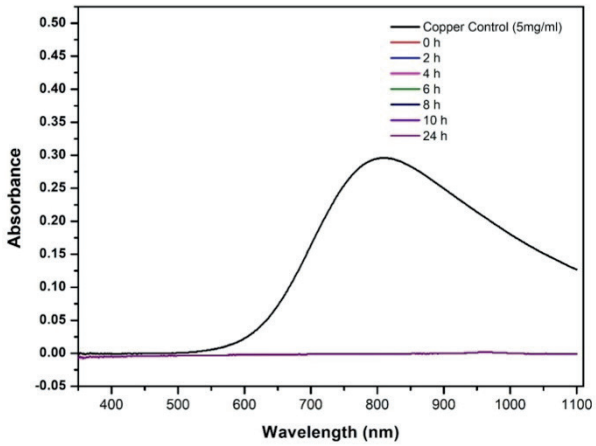

Figure S2. Leaching studies of copper nanoparticles

Antibacterial Activity of Copper Nanoparticles

The antibacterial activity assay has been investigated by the agar diffusion method. The nanoparticles synthesized using DAS has been used in the finishing process and nanoparticles synthesized using gallic acid has been used in the retanning

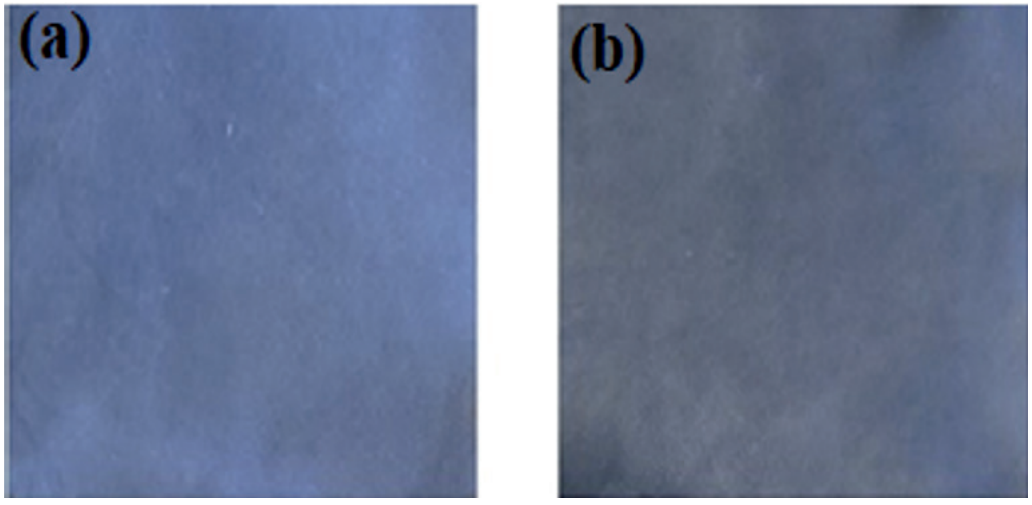

Figure 8. Photographic image of (a) control leather and (b) copper nanoparticles retanned leather

Table I

Color fastness values of control leather and leather finished using copper nanoparticles

Color fastness to rubbing	Control	Copper coated
Dry 512 rubs (material)	4/5	4/5
Wet 256 rubs (material)	4/5	4
Dry 512 rubs (felt)	4/5	4/5
Wet 256 rubs (felt)	4	4

Table II

L*a*b* values of control leather and leather retanned using copper nanoparticles

Values	Control	Experimental	Difference Δ
L*	99.78	88.17	11.61
a*	0.01	1.11	1.1
b*	0.06	9.95	9.89

Table III

Strength properties values of control leather and leather retanned using copper nanoparticles

Sample	Tensile strength (MPa)	Tear strength (N/mm)	Elongation at break (%)
Control	19.23 ± 0.5	52.27 ± 0.5	72.34 ± 0.5
Experiment	25.43 ± 0.5	71.39 ± 0.5	87.01 ± 0.5

Table IV

Color fastness values of control leather and leather finished using copper nanoparticles

Color fastness to rubbing – Greyscale	Control	Experiment
Dry 512 rubs (material)	4	4
Wet 256 rubs (material)	3/4	3/4
Dry 512 rubs (felt)	4/5	4/5
Wet 256 rubs (felt)	2	3

process. The antibacterial activity of copper nanoparticles coated leather was assessed by placing the leather samples on the agar surface against gram-positive and gram-negative bacteria. However, various mechanisms behind the bactericidal activity of metallic nanoparticles have been well studied earlier, commonly followed mechanism where an accumulation of nanoparticles in the bacterial membrane alters its cell permeability, with consequent release of LPS, membrane proteins, and intracellular components.[5] It is evident from Figures 9, 10, and 11 that the increasing concentration of copper nanoparticles effectively inhibits the growth of bacterial species both in the finished and retanned leather.

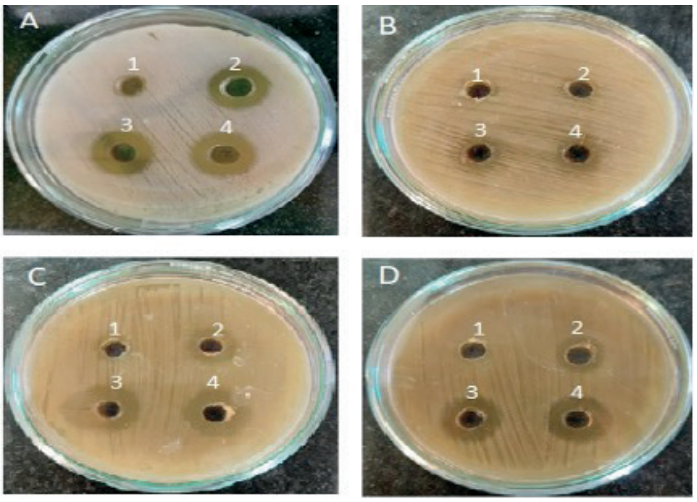

Figure 9. Effect of various concentrations of copper nanoparticles using DAS on growth inhibition zone of bacterial species (**A**- *B. cereus*, **B**- *S. aureus*, **C**- *E. coli,* and **D**- *P. aeruginosa*), 1- 10 % nanoparticles, 2- 20 % of nanoparticles, 3- 30 % of nanoparticles, 4- 40% of nanoparticles

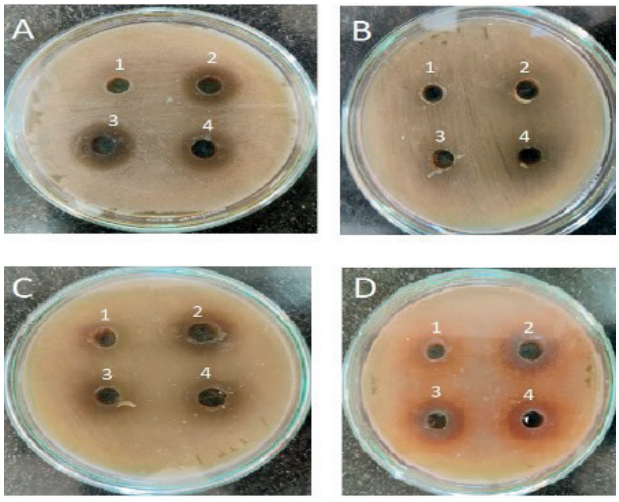

Figure 10. Effect of various concentrations of copper nanoparticles using gallic acid on growth inhibition zone against bacterial species (A- *B. cereus*, B- *S. aureus*, C- *E. coli,* and D- *P. aeruginosa*), 1- 10 % nanoparticles, 2- 20 % of nanoparticles, 3- 30 % of nanoparticles, 4- 40% of nanoparticles

Mechanism of Bacterial Killing

Changes in the bacterial cell membrane potential has been studied using 3', 3' diphenylthiocarbocyanine iodide. This is a non-fluorescent dye that binds with cell membrane protein and becomes fluorescent which can be quantified in a spectrofluorometer. The fluorescence intensity is directly proportional to the extension of cell lysis and alteration of cell membrane potential. It is evident from Figure 12 a that the copper nanoparticles cause modification of membrane potential in the bacterial cell wall and cause disruption of cytoplasm, which results in the increased fluorescence intensity due to the leached cells compared to the positive and negative control. Similarly, 2', 7' dichlorodihydrofluorescein diacetate (DCFHDA) is a reduced form of fluorescein commonly used as a marker for reactive oxygen species in cells. Copper nanoparticles disrupt the bacterial cell wall, resulting in the cleavage of membrane protein and increased generation of reactive oxygen species. The mechanism of this assay is that DCFHDA could easily cross the cell membrane and hydrolyze the diacetate groups by cytosolic

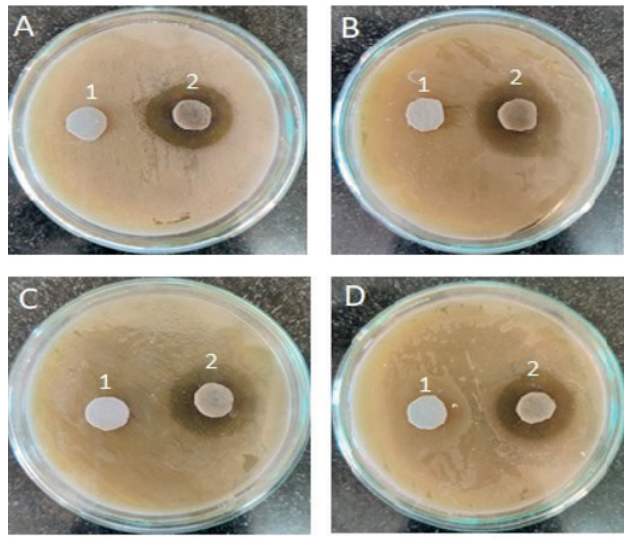

Figure 11. Effect of control finished leather and copper nanoparticles coated finished leather against bacterial species (A- *B. cereus*, B- *S. aureus*, C- *E. coli,* and D- *P. aeruginosa*)**,** 1- control leather, 2- nanoparticles coated leather.

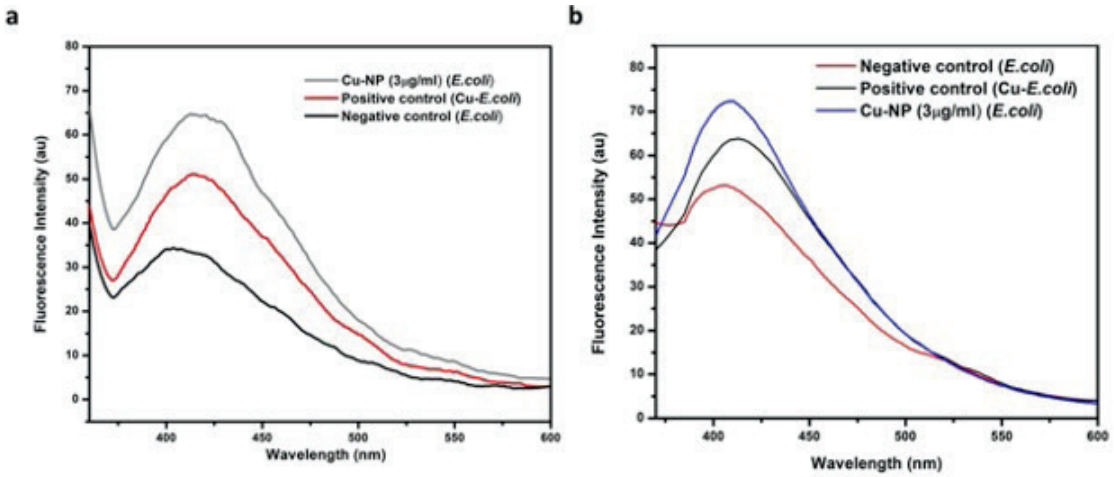

Figure 12. Fluorescence spectra of (a) *E. coli* bacterial cell membrane potential, (b) ROS generation in *E. coli* bacterial cell

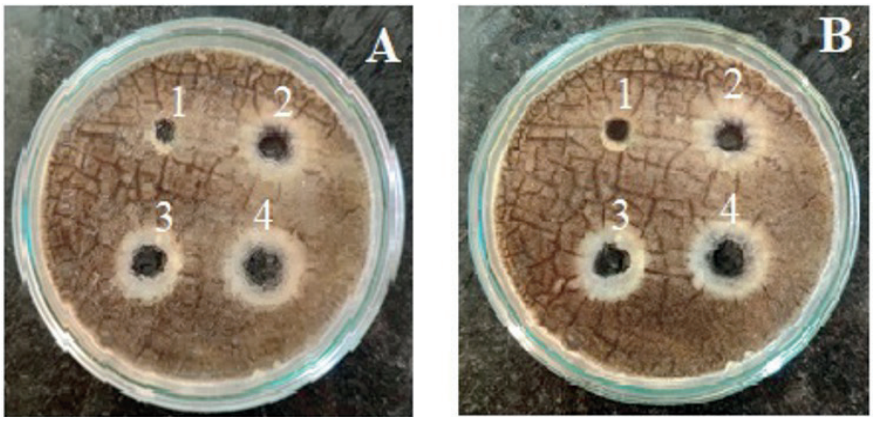

Figure 13. Growth inhibition zone of copper nanoparticles using (A) DAS and (B) gallic acid against *A. niger,* 1- 10 % nanoparticles, 2- 20 % of nanoparticles, 3- 30 % of nanoparticles, 4- 40% of nanoparticles

esterases; subsequently, DCDHF is oxidized by peroxynitrite to the highly fluorescent product dichlorofluorescein. Therefore, the fluorescence intensity of DCF is proportional to the ROS generation within cells. It is evident from Figure 12 b that there is an increased fluorescence intensity for the copper nanoparticles due to the increased production of reactive oxygen species compared to the positive control and negative control.

Antifungal activity of Copper Nanoparticles

The antifungal activity assay was investigated by the agar diffusion method. The zone of inhibition in the radius of copper nanoparticles synthesized has been measured against fungal species on the agar surface against *A. niger* as shown in Figure 13. The plausible mechanisms of action of copper ions and copper nanoparticles are based on altering the structure and function of the fungi cell; furthermore, these particles can affect DNA and disrupt its replication and transcription, ultimately leading to the death of fungal microorganisms.[21]

Conclusion

The current study deals with the synthesis of copper nanoparticles by chemical reduction method using dialdehyde starch and polyethylene diamine, sodium borohydride and gallic acid and applied in the finishing and retanning process, respectively. The nanoparticles retanned leather imparts both antimicrobial and functional properties such as good mechanical strength to the experiment leather. The fluorescence assay measurements clearly indicate the inhibitory efficiency of the nanoparticles in the bacterial cell. The nanoparticles coated leather finished leather effectively inhibits the growth of both bacterial and fungus growth. Thus, the present study paves the way for effectual utilization of nanoparticles in the leather process.

Conflict of Interests

No conflict of interest is associated with this manuscript.

Author Contributions

The manuscript was written through the contributions of three authors. All the authors have approved the final version of the manuscript.

Funding Information

Authors acknowledge CSIR-Central Leather Research Institute for financial support through the OLP-2313 project. The CLRI communication number is 1640.

References

1. Tarannum, A., Muvva, C., Rao, J R., Fathima, N N.; Phosphonium based ionic liquids-stabilizing or destabilizing agents for collagen, *RSC Advances* **6**, 4022-4033, 2016.
2. Sathish, M., Bhuvansewari, T S., Rao, J R., Fathima, N N.; Effect of Syntan to Fatliquor Ratio on Porosity and Mechanical Properties of Wet-blue Leather, *JALCA* **112**, 121-127, 2017.
3. Ocak, B., Yasa, I.; Antimicrobial activity of chrome-tanned leathers treated with chitosan formate, *Journal of the Society of Leather Technologists and Chemists* **99**, 238-244, 2015.
4. Bielak, E., Sygula, J.; Antimicrobial effect of lining leather fatliquored with the addition of essential oils, *Food Science and Biotechnology* **81**, 149-157, 2017.
5. Arijit, R., Ruchira, B.; Mechanism of antibacterial activity of copper nanoparticles, *Nanotechnology* **25**, 13-17, 2014.
6. Vincent, V., Duval, A.; Contact killing and antimicrobial properties of copper, *Journal of Applied Microbiology* **124**, 1032-1046, 2017.

7. Shankar, S.; Effect of copper salt and reducing agents on characteristics and antimicrobial activity of copper nanoparticles, *Materials Letters* **132**, 307-311, 2014.
8. Jayesh, J., Arup, T.; Strain specificity in antimicrobial activity of silver and copper nanoparticles, *Acta Biomaterialia* **4**, 707-716, 2008.
9. Ramkumar, S., Muthuraman, B.; A novel nano-finish formulations for enhancing performance properties in leather finishing applications, *Journal of Cluster Science* **27**, 1263-1272, 2016.
10. Khan, A.; A chemical reduction approach to the synthesis of copper nanoparticles, *International Nano Letters* **6**, 21-26, 2015.
11. Alba, D., Guajardo, G.; Antimicrobial properties of copper nanoparticles and amino acid chelated copper nanoparticles produced by using a soya extract, *Bioinorganic Chemistry and Applications* **2**, 1-6, 2017.
12. Bielak, E.; Investigation of finishing of leather for inside parts of the shoes with a natural biocide, *Scientific Reports Natural Research* **10**, 1-5, 2020.
13. Gongyan, G., Haiqi, F.; Fabrication of silver nanoparticle sponge leather with durable antibacterial property, *Journal of Colloid and Interface Science* **514**, 338-348, 2018.
14. Gongyan, G., Kaijun, K.; PEGylated chitosan protected silver nanoparticles as water-borne coating for leather with antibacterial property, *Journal of Colloid and Interface Science* **490**, 642-651, 2017.
15. Maestre, I., Federico, A.; Antimicrobial effect of coated leather based on silver nanoparticles and nanocomposites: synthesis, characterisation and microbiological evaluation, *Journal of Biotechnology & Biomaterials* **5**, 1-10, 2015.
16. Kushagri S, Kavita, K.; Antiviral and antimicrobial potentiality of nano drugs, *Micro and Nano Technologies,* 343-356, 2019.
17. Dou, Y., Zhang, B., He, M.; Preparation and physicochemical properties of dialdehyde Starch crosslinked feather keratin/PVA Composite Films, *Journal of Macromolecular Science Part A* **51**, 1009–1015, 2014.
18. Rohner, C., Pekkari, A., Harelind, H., Poulsen, K.; Synthesis of Cu nanoparticles: stability and conversion into Cu_2S nanoparticles by decomposition of alkane thiolate, *Langmuir* **33**, 13272–13276, 2017.
19. Mott, B., Galkowski, J., Wang, L., Luo, L., Chan, J.; Synthesis of size-controlled and shaped copper nanoparticles, *Langmuir* **23**, 5740-5745, 2007.
20. Zhen, L., Li, L.; Mild Synthesis of Copper nanoparticles with enhanced oxidative stability and their application in antibacterial films, *Langmuir* **34**, 14570-14576, 2018.
21. Diep, N., Duong, M., Le, M., Hoang, H., Oanh, L.; Preparation and characterization of antifungal colloidal copper nanoparticles and their antifungal activity against Fusarium oxysporum and Phytophthora capsica, *Comptes Rendus Chimie* **22**, 786-793, 2019.
22. Wu, S., Rajeshkumar, S., Madasamy, M., Mahendran, V.; Green synthesis of copper nanoparticles using Cissus vitiginea and its antioxidant and antibacterial activity against urinary tract infection pathogens, *Artificial Cells Nanomedicine, and Biotechnology* **48**, 1153-1158, 2020.
23 Wang, Y., Asefa, T.; Poly (allylamine)-stabilized colloidal copper nanoparticles: synthesis, morphology, and their surface-enhanced raman scattering properties, *Langmuir* **26**, 7469–7474, 2010.
24. Thanh, N., Maclean, N., Mahiddine, S.; Mechanisms of nucleation and growth of nanoparticles in solution, *Chemical Reviews* **114**, 7610–7630, 2014.
25. Fathima, N N., Rajaram, A., Sreedhar, B., Mandal, A B.; The formation of copper oxide nanorods in the presence of various surfactant micelles, *Indian Journal of Science and Technology* **1**, 1-6, 2008.
26. Mondal, P., Sinha, A., Salam, N., Roy, A S., Jana, N., Islam, M.; Enhanced catalytic performance by copper nanoparticle–graphene-based composite, *RSC Advances* **3**, 5615-5623, 2013.